Journal of Applied Mechanics and Technical Physics, Vol. 37, No. 3, 1996

ELONGATION FLOW OF A GRAVITATIONALLY BENT VISCOELASTIC JET

V. M. Shapovalov

UDC 532.522:532.135

The longitudinal flow of anomalous liquids is closely involved in the technology of forming of synthetic fibers and measurements of rheological properties [1]. Numerous papers are devoted to nontrivial hydrodynamic effects accompanying the flow of rectilinear jets [2, 3]. The steady-state flow of a nonrectilinear viscoelastic jet was first considered in [4].

In the present work, we study the longitudinal flow of a free jet under the transverse action of gravity forces. A new hydrodynamic phenomenon, namely, bifurcation of tensile stresses and of the stationary jet configuration, is found. The dynamic flow regimes are studied. The mechanism of generation of self-oscillations is explained.

1. Let us consider the main features of steady-state flow. The flow and the balance of forces acting on an elementary section of the flow are shown schematically in Fig. 1. The liquid is fed at a constant velocity v_0 from a filler. From the flow region the jet is uniformly collected by an intake receiver (suction roll), which specifies a certain value of the longitudinal velocity v_1. The x axis is directed horizontally. The outflow and collection points are located at the same level. The origin of the Eulerian coordinate system is placed in the section in which profile rearrangement has been completed. The jet and the coordinate axes lie in one vertical plane. The air drag and surface tension of the liquid are ignored. We assume that viscous forces are so great that inertial effects and capillary forces are negligible in comparison. An element of the jet experiences the effect of gravity and rheological resistance.

Description will be performed within the framework of quasi-one-dimensional equations of continuity and conservation of momentum:

$$\frac{\partial a^2}{\partial t} + \frac{\partial a^2 v}{\partial s} = 0, \quad \frac{\partial}{\partial s}(P\cos\varphi) = 0, \quad \frac{\partial}{\partial s}(P\sin\varphi) = \pi a^2 \rho g, \quad P = \pi a^2 \sigma_{11}. \tag{1.1}$$

Here s is the coordinate reckoned along the jet axis; P is the tension force in the normal section; a is the current radius of the round jet; σ_{11} is the tensile stress; ρ is the liquid density; g is the acceleration of gravity; v is the axial velocity; and φ is the angle of inclination of the jet to the horizontal.

We write the boundary conditions for steady-state flow as

$$x = 0, \quad y = 0, \quad \varphi = \varphi_0, \quad v = v_0, \quad a = a_0; \quad x = l, \quad y = 0, \quad v = Kv_0, \tag{1.2}$$

where l is the length of the flow zone; $K = v_1/v_0$ is the stretching multiplicity; a_0 is the initial radius; and φ_0 is the initial angle.

To close the problem, Eqs. (1.1) should be supplemented by the dependence of tensile stresses on the strain rate. Conventionally, polymer solutions and melts are subjected to uniaxial tension under isothermal and anisothermal conditions, however, the main features of the flow in question are found already in the Newton approximation. Under uniaxial tension of a Newtonian fluid the stress is determined from the formula

$$\sigma_{11} = 3\eta \frac{\partial v}{\partial s} \tag{1.3}$$

where η is the viscosity.

Volgograd State Technical University, Volgograd 400103. Translated from Prikladnaya Mekhanika i Tekhnicheskaya Fizika, Vol. 37, No. 3, pp. 58–66, May–June, 1996. Original article submitted March 9, 1995.

 0021-8944/96/3703-0350 $15.00

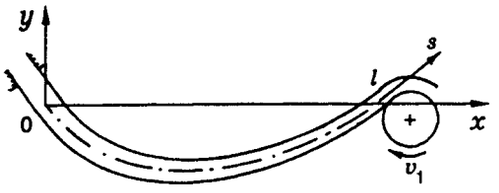

Fig. 1

Integrating the second equation in (1.1), we obtain $P\cos\varphi = H(t)$. Consequently, the horizontal tension component H is uniform along the jet and can vary with time only in dynamic regimes. Let us consider preliminarily the case of steady flow, in which, instead of the first equation in (1.1), we use the integral continuity condition $va^2 = v_0a_0^2$.

Introduction of the dimensionless variables

$$X = \frac{x}{l}, \quad Y = \frac{y}{l}, \quad V = \frac{v}{v_0}, \quad q = \frac{Hl}{3\eta\pi a_0^2 v_0}, \quad R = \frac{\rho g l^2}{3\eta v_0} \tag{1.4}$$

enables us to write problem (1.1)–(1.3) for steady-state conditions in the form

$$\frac{dY}{dX} = \tan\varphi, \quad \frac{d\varphi}{dX} = \frac{R\cos\varphi}{qV}, \quad \frac{dV}{dX} = \frac{qV}{\cos^2\varphi},$$
$$X = 0, \quad Y = 0, \quad \varphi = \varphi_0, \quad V = 1; \quad X = 1, \quad Y = 0, \quad V = K. \tag{1.5}$$

We used the obvious relations $ds\cos\varphi = dx$, $ds\sin\varphi = dy$.

The solution of problem (1.5) in quadratures has the form

$$X = \frac{q}{R}\int_{z_0}^{z} \frac{V dz}{\sqrt{1+z^2}}, \quad Y = \frac{q}{R}\int_{z_0}^{z} \frac{V z dz}{\sqrt{1+z^2}}, \quad z = \tan\varphi, \quad z_0 = \tan\varphi_0,$$

$$\frac{2R}{q^2}(1 - V^{-1}) = z\sqrt{1+z^2} - z_0\sqrt{1+z_0^2} + \operatorname{Arsinh} z - \operatorname{Arsinh} z_0.$$

Problem (1.5) was analyzed using the fourth-order Runge–Kutta method. For given R and q the conditions at the collection point $X = 1$, $Y = 0$ were fulfilled by varying the parameter φ_0 (the shooting method). In so doing, the stretching multiplicity $K = V(X = 1)$ was determined.

The results of the analysis are presented in Fig. 2. For the gravitational parameter $R = 0$, 5, 10, 20, and 40 (curves 1–5, respectively) the curves of dimensionless tension (a) and of the deflection of the jet middle part $Y_m = Y(X = 0.5)$ versus the multiplicity (b) are shown. One can see that to fixed K and R correspond two values of the tensile stress q and two significantly different values of the deflection. A reduction of the multiplicity (decrease in the suction rate) causes the values of q and Y_m to approach the degeneration point of bifurcation, below which steady flow is impossible. Deflections $Y_m \approx -0.35$ correspond, practically independently of R, to critical multiplicities. Flows with small deflections ($Y_m \geqslant -0.35$) are called subcritical, and flows with great deflections, supercritical. The line $R = 0$ is described by the equations $K = \exp(q)$ and $Y_m = 0$.

The above flow regimes differ significantly in their responses to changes in the flow parameters, as illustrated in Table 1. Thus, an increase in the suction rate decreases the deflection in subcritical flow and increases it in supercritical flow. An increase in the acceleration of gravity or in the length of the flow zone increases the deflection in subcritical flow and decreases it in supercritical flow.

The phenomenon of bifurcation was observed on a technological setup for horizontal forming of a flat polymer film from a polypropylene melt. The flow pattern was similar to that presented in Fig. 1. Traditionally, the forming process is carried out by small deflections of the jet (subcritical regime). An increase in the length

TABLE 1

Regime	Variation of flow parameters			
	$-Y_m$	dK/dq	$d\|Y_m\|/dR$	$d\|Y_m\|/dK$
Subcritical	$\leqslant 0.35$	>0	>0	<0
Critical	≈ 0.35	0	0	0
Supercritical	$\geqslant 0.35$	<0	<0	>0

of the flow zone (by means of horizontal displacement of the suction roll) results in smooth transition of the jet to a critical regime, which manifests itself in progressive downward displacement of the jet. After the initial length of the flow zone was restored, the jet did not return to the previous position but remained in the region of great (supercritical) deflections, preserving flow stability. For high-viscosity liquids (polyisobutylene solutions, molasses) the existence of critical multiplicities of stretching and deflections is confirmed under laboratory conditions. We were unable to realize steady supercritical flow under isothermal conditions, probably because of the low density of the jet at the suction point.

2. To obtain a comparative estimate of the stability of the flows found, we studied dynamic regimes by introducing perturbations of different intensity. To close problem (1.1), we use the Maxwell rheological equation of a generalized fluid [5]:

$$\tau + \lambda \frac{D_0 \tau}{D_0 t} = 2\eta d.$$

Here λ is the relaxation time; d is the strain rate tensor; τ is the stress tensor deviator; and D_0/D_0t is the Oldroid convective derivative. For a Newtonian fluid, $\lambda = 0$.

Calculations were carried out for the case of the higher convective derivative. Under uniaxial tension, axial stresses are described by the equation

$$\sigma_{11}\left(1 - 2\lambda \frac{\partial v}{\partial s}\right) + \lambda v \frac{\partial \sigma_{11}}{\partial s} = 3\eta \frac{\partial v}{\partial s}. \tag{2.1}$$

The initial and boundary conditions for Eqs. (1.1), (1.2) are as follows:

$$\begin{gathered} t = 0: \quad a = a_*(x), \quad v = v_*(x), \quad y = y_*(x), \\ t > 0: \quad x = 0, \quad v = v_0, \quad y = 0, \quad a = a_0, \\ t > 0: \quad x = l, \quad v = Kv_0, \quad y = 0. \end{gathered} \tag{2.2}$$

In (2.2) and below the asterisk denotes variables and parameters that correspond to steady flow.

The steady flow of a viscoelastic jet is described by the following system of equations:

$$\begin{gathered} \frac{dY_*}{dX} = \sinh \xi_*, \quad \frac{d\xi_*}{dX} = \frac{R}{qV_*}, \quad \frac{dV_*}{dX} = \frac{V_*(q_* \cosh^2 \xi_* + \mathrm{We}\, R \sinh \xi_*)}{1 + \mathrm{We}\, q_* V_* \cosh \xi_*}, \quad r_*^2 V_* = 1, \\ X = 0, \quad Y_* = 0, \quad V_* = 1, \quad \xi_* = \xi_{*0}; \quad X = 1, \quad Y_* = 0, \quad V_* = K, \end{gathered} \tag{2.3}$$

where $\tau = tv_0/l$; $r = a/a_0$; and $\mathrm{We} = \lambda v_0/l$.

The unsteady flow problem was solved numerically without linearization. First we found a steady solution of (2.3). The unsteady solution was presented in the form

$$r = r_*(X)[1 + \alpha(X,\tau)], \quad V = V_*(X)[1 + \beta(X,\tau)], \quad Y = Y_*(X) + \gamma(X,\tau). \tag{2.4}$$

From Eqs.(1.1) and (2.1), taking into account (1.4), (2.3), and (2.4), we obtain equations for the deflections:

$$F_1 = \frac{1}{\cosh \zeta} V_*(1 + \beta), \quad F_2 = -\frac{1}{2\cosh \zeta} V_*(1 + \alpha) F_3, \tag{2.5}$$

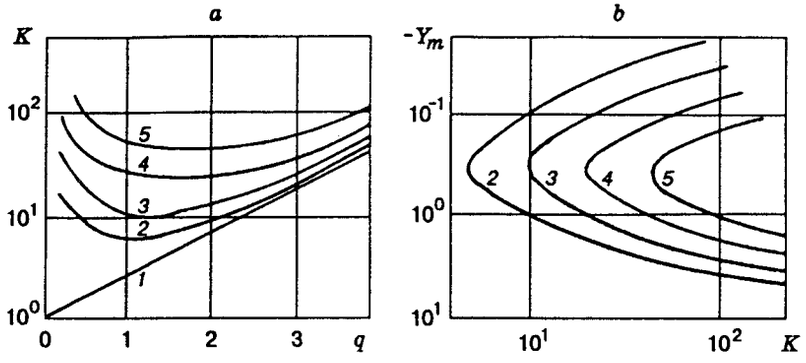

Fig. 2

$$F_3 = \frac{q\cosh^2\zeta + \mathrm{We}\,R\sinh\zeta}{(1+\alpha)^2 + \mathrm{We}\,qV_*\cosh\zeta} - (1+\beta)\frac{q_*\cosh^2\xi_* + \mathrm{We}\,R\sinh\xi_*}{1 + \mathrm{We}\,q_*V_*\cosh\xi_*}.$$

The conditions for the deflections in the case of disturbance of the initial radius or velocity are written as

$$\begin{gathered} \tau = 0: \quad \alpha = \beta = \gamma = 0, \quad \zeta = \xi_*(X), \\ \tau > 0: \quad X = 0, \quad \alpha = \alpha_0, \quad \beta = \beta_0, \quad \gamma = 0, \quad \zeta = \zeta_0(\tau), \\ \tau > 0: \quad X = 1, \quad \beta = \gamma = 0. \end{gathered} \tag{2.6}$$

The dynamic regimes are identical under velocity disturbances in the initial or outlet cross-section [6]. The tensile stresses q_* and $q(\tau)$ are uniform along the jet.

Within each "time layer" the equations for β, γ, and ζ were solved by the fourth-order Runge–Kutta method, since we have the Cauchy problem for the system of three first-order equations. The parameters q and ζ_0 were chosen from the conditions $\beta(X = 1, q, \zeta_0) = 0$ and $\gamma(X = 1, q, \zeta_0) = 0$, which were treated as a system of transcendental equations. The roots were found using a secant–chord algorithm. To render the one-dimensional equation of convective transfer discrete, we used the Crank–Nicolson finite-element scheme [7] with approximation order $O(\Delta\tau^2, \Delta X^4)$ realized by a three-point sweep. Here $\Delta\tau$ and ΔX are the time step and step for X, respectively.

We considered the dynamic regimes of a viscous fluid (We $= 0$) for steady flows with close stretching multiplicity and identical gravitational parameters $R = 5$: subcritical flow for $q_* = 1.5$, $\xi_*(X = 0) = -0.928$, $Y_{*m} = -0.181$, and $K = 5.98$ and supercritical flow for $q_* = 0.5$, $\xi_*(X = 0) = -2.252$, $Y_{*m} = -0.628$, and $K = 5.76$. The value $R = 5$ corresponds to the critical regime with $q_* = 0.922$, $\xi_*(X = 0) = -1.49$, $Y_{*m} = -0.341$, and $K = 4.74$.

Figure 3 presents the kinetics of displacement of the middle part of the jet $Y_m = Y_{*m}(1 + \gamma_m)$ [$\gamma_m = \gamma(X = 0.5)$ and $Y_{*m} = Y_*(X = 0.5)$] during stepwise disturbances of the initial radius for $\alpha_0 \neq 0$ and $\beta_0 = 0$ (a) and initial velocity for $\alpha_0 = 0$ and $\beta_0 \neq 0$ (b). In Fig. 3a, curves 1–8 correspond to $\alpha_0 = 0.2$, 0.25, -0.5, -0.6, 0.5, 0.6, -0.55, and -0.7. In Fig. 3b, curves 1–8 correspond to $\beta_0 = 0.8$, 0.85, -0.6, -0.7, 0.6, 1.1, -0.6, and -0.95. The circles correspond to loss of stability. It is evident that immediately before loss of stability the jet moves to regions of critical deflection (curves 2, 4, 6, and 8 in Fig. 3a and 2 and 4 in Fig. 3b).

When the radius is disturbed in subcritical flow, rapidly attenuating longitudinal waves of contraction and distention propagate along the jet. When $\alpha_0 > 0$, jet necking starts near the suction point, and the deflection increases. It is during the necking of the outlet section that loss of stability takes place for $\alpha_0 \geqslant 0.25$ and $\tau \approx 0.2$. When $\alpha_0 < 0$, loss of stability can occur in the period $\tau \approx 0.6$ due to contraction of the jet outlet section. Over the initial periods the outlet section increases.

When the initial radius is disturbed, vertical deflections of the jet (from the position of static equilibrium) in supercritical flow are greater than in critical flow. The duration of the transient processes

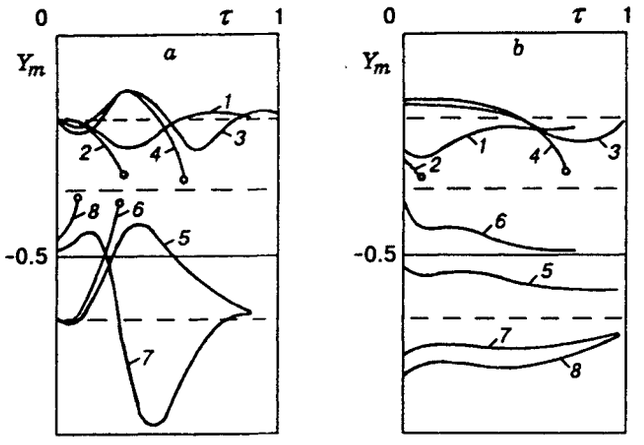

Fig. 3

also increases owing to the greater extension of the jet. When $\alpha_0 \geqslant 0.6$, loss of stability occurs at the moment $\tau \approx 0.27$ and is due to progressive tapering of the jet near $X \approx 0.8$. When $\alpha_0 \leqslant -0.7$, the loss of stability is due to tensile strains in the vicinity of the initial section. On completion of the transient processes the following relations are characteristic of the new steady flow: $\alpha = \alpha_0$, $\beta = \gamma = 0$, $\partial\alpha/\partial\tau = 0$, $\partial\alpha/\partial X = 0$, $\zeta = \xi_*$, and $q = q_*(1 + \alpha_0)^2$.

In the case of disturbance of the initial velocity, the tension and deflection of the jet change stepwise. The distribution of velocity disturbances is nearly linear and varies only slightly during the transient process. The supercritical flow is rather stable against negative velocity disturbances: the flow was maintained even at $\beta_0 = -0.95$.

Even small disturbances of the radius or velocity in the critical flow ($\alpha_0 \approx \beta_0 \approx \pm 0.01$) cause rapid loss of stability of the finite-difference scheme in the first time steps.

Thus, the subcritical and supercritical regimes are comparable in stability to disturbances in the initial section.

A similar analysis was performed for a viscoelastic liquid. In the subcritical regime the disturbances lead to an insignificant vertical displacement of the jet. The flow stability increases significantly. On the whole, the "damping" properties of the system, which manifest themselves in a reduction in the oscillation amplitude of the middle part of the jet and in rapid attenuation of transient processes, are considerably increased. However, self-oscillations which bring about loss of stability appear in the supercritical regime for $\alpha_0 < -0.2$.

For a viscoelastic liquid, a numerical experiment on transition from subcritical to supercritical flow by varying the parameter R (which is equivalent to variation of the length of the flow zone) was carried out. The characteristics of the steady subcritical flow were as follows: $R = 5$, We $= 0.1$, $q_* = 15$, $K = 9.5$, $\xi_{*0} = -0.0644$, and $Y_{*m} = -0.0985$. The program of variation of the parameter R and of the deflections of the middle part of the jet is shown in Fig. 4. The parameter R was varied stepwise interactively after every two time steps. The initial step for R was 5, but as critical deflections were approached, the step was decreased gradually to 0.02 (horizontal plateau is shown for $0.15 < \tau < 0.3$ in Fig. 4). The value $R = 37.5$ corresponds to critical deflections. The time of transition of the flow to the supercritical regime was determined by the character of the dependence of deflection on R (see Table 1). After the transition the gravitational parameter reduces to 5. In this case, the deflection increased, approaching the steady supercritical regime.

As R increases in the subcritical flow, the jet is shifted downward, its cross-section in the middle part increases, and, accordingly, the initial and outlet sections decrease. Then, on the plateau $R \approx 37.5$ the distention wave is shifted to the suction point. It is this "strengthening"of the outlet section that makes possible further transition to supercritical flow and prevents jet cutoff. The latter causes difficulties in realizing the transition for a Newtonian fluid.

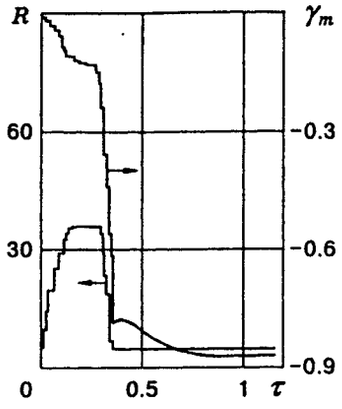

Fig. 4

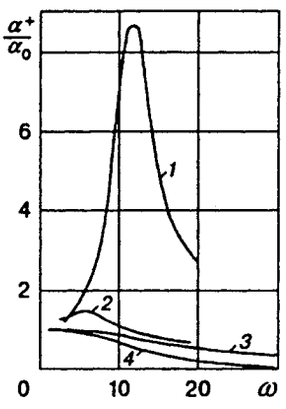

Fig. 5

Thus, the bifurcation phenomenon is consistent with the uniqueness of the solution of the Navier–Stokes equations [8], since the flow regime depends uniquely on the implementation of the process (sequence of operations), i.e., on the initial conditions.

The effect of the elastic properties on the amplitude-frequency characteristic of the system was studied numerically. In the case of harmonic disturbances of the initial radius, the boundary conditions for (2.5) are as follows: $X = 0$, $\alpha = \alpha_0 \sin \omega\tau$, $\beta = \gamma = 0$, and $\zeta = \zeta_0$; $X = 1$ and $\beta = \gamma = 0$, where $\omega = \omega^0 l/v_0$; ω^0 is the frequency.

The region of moderate frequencies is considered in the vicinity of the inverse time of stay of an element of volume in the deformation zone. The amplitude of disturbances is $\alpha_0 \leqslant 0.1$. The amplitude of oscillations of the outlet radius was monitored after establishment of the oscillation regime α^+. The subcritical and supercritical regimes for viscous ($K = 5.98$ and $R = 5$) and viscoelastic ($K = 9.5$, $R = 5$, and We $= 0.1$) liquids are studied.

Figure 5 presents the amplitude-frequency characteristics. The amplification factor α^+/α_0 is plotted along the x-axis. Curves 1 and 2 correspond to subcritical and the supercritical viscous flows, while 3 and 4, to subcritical and the supercritical viscoelastic flows.

In subcritical viscous flow, the dependence is of a clearly expressed resonance character. In the resonance region the curve of $\alpha(X = 1, \tau)$ has pointed maxima similar to those described in [9]. Vertical oscillations of the middle part of the jet are also of a resonance character. In supercritical flow, the "damping" properties of the jet increase and the eigenfrequency decreases. There are considerable vertical resonance oscillations of the middle part of the jet. The viscoelastic liquid possesses clearly expressed "damping" properties, and the amplification of disturbances decreases significantly for all moderate frequencies in both regimes. Numerical study of short-wave disturbances ($\omega \gg 1$) makes no sense, because long-wave approximation equations are used.

The influence of jet nonrectilinearity on "resonance under stretching" is analyzed. It is known that for rectilinear viscous jets self-oscillations of finite radius with increasing amplitude occur when $K > 20$ and 22 [10, 11]. It was noted in [10] that the finite-difference approximation for rectilinear jets gives an overestimated critical multiplicity. Therefore, the results presented below permit one to estimate only qualitatively the effect of flow conditions on the generation of self-oscillations.

For a viscous liquid (We $= 0$) a stepwise disturbance of the initial velocity $\beta_0 = 0.05$ and $\alpha_0 = 0$ was assigned in (2.6). For fixed R, as q_* increases [in this case multiplicity was determined from the steady-state problem (2.3)] the moment of appearance of self-oscillations of the outlet radius of increasing amplitude was noted in the system. If the effect of gravitation is slight ($R = 1$ and $Y_{*m} = -0.0034$) for $q_* < 4.9$ ($K < 134$) the oscillations attenuate, and for $q_* > 4.9$ ($K > 134$) sinusoidal self-oscillations of increasing amplitude are established. Normal bifurcation of cycle generation takes place. As the jet deflection increases within

critical deflections ($R = 20$ and $Y_{*m} = -0.058$) self-oscillations with increasing amplitude appear at $q_* > 5.05$ ($K > 183$). An increase in the gravitational parameter R from 1 to 20 is equivalent to an increase in the flow zone by a factor of $\sqrt{20}$. Thus, a small deflection of the stretched jet increases its stability against the appearance of self-oscillations. With increasing R, the value of q_* corresponding to the moment of generation of self-oscillations increases insignificantly.

For a fixed R, the tendency of longitudinal flow to manifest of self-oscillations is studied in a wide range of deflections. According to Fig. 2, the steady-state deflection is uniquely determined by q_*. As was mentioned above, self-oscillations occur for small deflections (comparatively great K and q_*). As the deflections increase, self-oscillations appear near the critical flow regime $Y_* \approx -0.3$ (parametric resonance). No self-oscillations are found in the supercritical regime. With an increase in the deflections the character of variation in the outlet radius changes gradually from oscillatory to aperiodically attenuating. Therefore, the flow instability in critical deflections is due to the appearance of increasing-amplitude self-oscillations in the jet. This causes difficulties in the transition of subcritical flow to the supercritical regime.

In the flow under consideration the spontaneous intensification of oscillations is caused by an additional energy supply to the jet. The generation of increasing-amplitude self-oscillations is characteristic of feedback systems [12]. Information on the changing outlet radius returns to the flow zone as a tensile stress of uniform length which changes with time (capillary and inertial forces are ignored). The pulsations of tensile stress exert a modulating effect on the dynamic processes in the jet. In isothermal viscous flows the strain rate gradient at the suction point takes the largest value, whereas the tensile stress is determined by $\pi a^2 \eta \partial v/\partial s$. Anisothermicity, dilatancy, and elastic properties reduce the tension rate gradient in the outlet section, and the steady flow region is widened. The feedback of tensile stress is eliminated in the case of stretching regime with a constant tensile stress, and no "resonance under tension" appears [2].

The author expresses gratitude to V. M. Entov for consideration of the work.

REFERENCES

1. A. Zyabitskii, *Theoretical Principles of Fiber Forming* [in Russian], Khimiya, Moscow (1979).
2. V. M. Entov and A. L. Yarin, "Dynamics of free jets and films and rheologically complicated liquids," *Itogi Nauki Tekh., Mekh. Zhidk. Gaza*, **18**, 112–197 (1984).
3. Z. P. Shul'man and B. M. Khusid, *Unsteady Processes of Convective Transport in Hereditary Media* [in Russian], Nauka Tekh., Minsk (1983).
4. V. M. Entov, S. M. Makhkamov, and K. V. Mukuk, "One effect of normal stresses," *Inzh.-Fiz. Zh.*, **34**, No. 3, 514–518 (1978).
5. G. Astarita and G. Marucci, *Principles of Non-Newtonian Fluid Dynamics* [Russian translation], Mir, Moscow (1978).
6. V. L. Kolpashchikov, O. G. Martynenko, and A. I. Shnip, "Dynamic model of response of the extension process of fiberglass to disturbances," *Inzh.-Fiz. Zh.*, **47**, No. 5, 817–822 (1984).
7. C. A. J. Fletcher, *Computational Techniques for Fluid Dynamics* [Russian translation], Mir, Moscow (1991), Vol. 1.
8. D. D. Joseph, *Stability of Fluid Motions* [Russian translation], Mir, Moscow (1981).
9. A. L. Yarin, "Effect of heat removal on unsteady regimes of fiber forming," *Inzh.-Fiz. Zh.*, **50**, No. 5, 810–818 (1986).
10. A. L. Yarin, "Appearance of self-oscillations during fiber forming," *Prikl. Mat. Mekh.*, **47**, No. 1, 82–88 (1983).
11. V. S. Berman and A. L. Yarin, "Dynamic regimes of fiber forming," *Izv. Akad. Nauk SSSR, Mekh. Zhidk. Gaza*, No. 6, 31–37 (1983).
12. N. Wiener, *Cybernetics or Control and Communication in the Animal and the Machine*, The Technology Press and John Wiley and Sons, Inc., New York–Herman et Cie, Paris (1948).